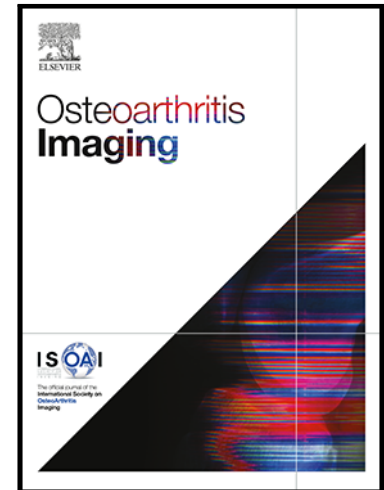


Journal Pre-proof

Multiparametric 3-D analysis of bone and joint space width at the knee from weight bearing computed tomography



Tom D Turmezei FRCR MPhil MA BMBCh PhD ,
Samantha B Low FRCR BEng MBBS , Simon Rupret Dr.med ,
Graham M Treece MA PhD , Andrew H Gee MA PhD ,
James W MacKay FRCR MBBChir PhD , John A Lynch PhD ,
Kenneth ES Poole MRCP BM PhD , Neil A Segal MD MS

PII: S2772-6541(22)00065-4
DOI: <https://doi.org/10.1016/j.ostima.2022.100069>
Reference: OSTIMA 100069

To appear in: *Osteoarthritis Imaging*

Received date: 30 December 2021
Revised date: 5 May 2022
Accepted date: 13 June 2022

Please cite this article as: Tom D Turmezei FRCR MPhil MA BMBCh PhD , Samantha B Low FRCR BEng MBBS , Simon Rupret Dr.med , Graham M Treece MA PhD , Andrew H Gee MA PhD , James W MacKay FRCR MBBChir PhD , John A Lynch PhD , Kenneth ES Poole MRCP BM PhD , Neil A Segal MD MS , Multiparametric 3-D analysis of bone and joint space width at the knee from weight bearing computed tomography, *Osteoarthritis Imaging* (2022), doi: <https://doi.org/10.1016/j.ostima.2022.100069>

This is a PDF file of an article that has undergone enhancements after acceptance, such as the addition of a cover page and metadata, and formatting for readability, but it is not yet the definitive version of record. This version will undergo additional copyediting, typesetting and review before it is published in its final form, but we are providing this version to give early visibility of the article. Please note that, during the production process, errors may be discovered which could affect the content, and all legal disclaimers that apply to the journal pertain.

© 2022 Published by Elsevier Ltd on behalf of International Society of Osteoarthritis Imaging.
This is an open access article under the CC BY-NC-ND license
(<http://creativecommons.org/licenses/by-nc-nd/4.0/>)

TITLE PAGE

Multiparametric 3-D analysis of bone and joint space width at the knee from weight bearing computed tomography

AUTHORS

Tom D Turmezei FRCR MPhil MA BMBCh PhD^{1,2*}

Samantha B Low FRCR BEng MBBS²

Simon Rupret Dr.med³

Graham M Treece MA PhD⁴

Andrew H Gee MA PhD⁴

James W MacKay FRCR MBChir PhD^{1,2}

John A Lynch PhD⁵

Kenneth ES Poole MRCP BM PhD⁶

Neil A Segal MD MS⁷

AFFILIATIONS

1 Norfolk and Norwich University Hospital NHS Foundation Trust, Colney Lane, Norwich, UK

2 University of East Anglia, Norwich Research Park, Norwich, UK

3 University Hospitals Bristol and Weston NHS Foundation Trust, Marlborough Street, Bristol, UK

4 Cambridge University Engineering Department, Trumpington Street, Cambridge, UK

5 University of California San Francisco, 550 16th Street, San Francisco, USA

6 University of Cambridge Department of Medicine, Hills Road, Cambridge, UK

7 University of Kansas Medical Center, 3901 Rainbow Boulevard, Kansas City, USA

*Corresponding author email: tom.turmezei@nnuh.nhs.uk

ABSTRACT[^] (250 words)

Objective

Computed tomography (CT) can deliver multiple parameters relevant to osteoarthritis. In this study we demonstrate that a 3-D multiparametric approach at the weight-bearing knee with cone beam CT is feasible, can include multiple parameters from across the joint space, and can reveal stronger relationships with disease status when parameters are combined.

Design

Weight-bearing (WBCT) images of the knees of 33 participants were analyzed with joint space mapping and cortical bone mapping to deliver joint space width (JSW), subchondral bone plate thickness, endocortical thickness, and trabecular attenuation on both sides of the joint. All data were

[^] Abbreviations: CBCT = cone beam CT; CBM = cortical bone mapping; CT = computed tomography; ET = endocortical thickness; HR-pQCT = high resolution peripheral quantitative CT; JSM = joint space mapping; JSW = joint space width; KLG = Kellgren and Lawrence grade; pQCT = peripheral quantitative CT; SPM = statistical parametric mapping; ST = subchondral thickness; TA = trabecular attenuation; WBCT = weight bearing CT.

co-localized to the same canonical surface. Statistical parametric mapping (SPM) was applied in uni- and multivariate models to demonstrate significant dependence of parameters on Kellgren & Lawrence grade (KLG). Correlations between JSW and bony parameters and 2-week test-retest repeatability were also calculated.

Results

SPM revealed that the central-to-posterior medial tibiofemoral joint space was significantly narrowed by up to 0.5 mm with significantly higher tibial trabecular attenuation — up to 50 attenuation units for each increment in KLG as a single parameter — and in a wider distribution when combined with others ($p < 0.05$). They were also more strongly correlated with worsening KLG grade category. Test-retest repeatability was subvoxel (0.37 mm) for nearly all thickness parameters.

Conclusions

3-D JSW and tibial trabecular attenuation are repeatable and significantly dependent on radiographic disease severity at the weight-bearing knee joint and even more so in combination. A quantitative multiparametric approach with WBCT may have potential for more sensitive investigation of disease progression in osteoarthritis.

KEYWORDS

Computed tomography; weight bearing; knee osteoarthritis; joint space width; subchondral bone; test-retest repeatability.

INTRODUCTION

Multiparametric imaging in osteoarthritis is usually considered the reserve of MRI, with measurement of T2 and T1rho half-life values, perfusion on dynamic contrast-enhanced MRI, and cartilage morphology recognized as relevant to disease [1]. Other parameters, however, can be quantitatively derived from CT imaging, such as bone mineral density, cortical bone thickness, cartilage thickness on arthrography, joint space width (JSW) on weight bearing, and shape [2–5].

In vivo techniques in the CT family including peripheral quantitative CT (pQCT), high-resolution pQCT (HR-pQCT), multidetector helical CT, cone beam CT (CBCT), dual energy and spectral CT, are also used to measure multiple parameters from a single acquisition. Karhula *et al.* in 2020, for example, explored subvoxel estimation of bone morphometric parameters from CBCT in comparison to microCT and histological analysis [6]. Other recent studies have looked at simultaneous quantification of bone mineral density and cartilage thickness using contrast-enhanced HR-pQCT and CT [7,8].

Although there are recognized associations, the behavior of bone in relation to developing osteoarthritis remains poorly understood; one cross-modality study found subchondral bone plate differences between injured and contralateral non-injured knees with HR-pQCT that had shown no

difference in cartilage distribution on MRI [9]. Yet joint space narrowing and subchondral bone sclerosis are widely accepted markers of the osteoarthritic joint.

The evolving capabilities of CT present an opportunity to define its role in establishing relationships between the natural history of osteoarthritis and imaging features of disease, in particular those it can depict as well as or better than other modalities. If CT output can be harnessed appropriately, it could prove to be a time- and cost-efficient alternative to MRI for assessing disease progression, and a more sensitive and reliable modality than radiography in the setting of osteoarthritis research trials and the clinic. It is worth noting that CBCT has a much lower radiation dose than traditional helical multidetector CT, and of course, it can be applied to weight-bearing knees.

Having already established that 3-D quantification with weight-bearing CT (WBCT) might be more sensitive to changes in JSW than radiography [4], CT might also be similarly used to assess the phenomenon of bony sclerosis that has been difficult to quantify. Here we revisit a previous analysis of JSW but now combine it with a new 3-D assessment of adjacent subchondral bone at the knee joint from a single WBCT acquisition. Our hypothesis was that a quantified 3-D multiparametric approach across the weight-bearing knee joint was feasible, and would allow investigation into the correlation of these features, which might reveal stronger relationships with disease severity than single parameters alone. We also demonstrate the test-retest repeatability for all these parameters, an important metric for understanding their ability to detect meaningful change against day-to-day variations in imaging acquisition.

METHODS

Participants for this study were from two separate knee WBCT studies performed between 2014 and 2018. [4]. The first convenience sample was from 23 individuals in the Multicenter Osteoarthritis Study from 2016 to 2018 who were involved in a prior study comparing WBCT with radiographic JSW [10]. Participants were recruited to the Multicenter Osteoarthritis Study, which had The University of Iowa institutional review board approval for demographic data collection (approval number 20003064) and WBCT image acquisition (approval number 201602741; all approved under FWA00003007). All participants provided informed consent prior to enrolment. The second convenience sample included 10 individuals recruited between June and August of 2014 for another study looking at the test–retest repeatability of a different JSW measurement method [11]. For that study, The University of Iowa institutional review board approval (no. 201403723) was obtained in conjunction with informed oral consent from all participants.

There were thus 33 individuals who had both knees imaged simultaneously in a 20-degree fixed-flexion position with the same prototype commercial CBCT imaging system (LineUp; CurveBeam). Images from the first visit were used from the second sample in the statistical parametric mapping (SPM) study, with follow-up imaging for repeatability analysis performed at a second visit 2 weeks later. The Kellgren & Lawrence grade (KLG) scores for all 66 knees were KLG 0 = 31, KLG 1 = 12,

KLG 2 = 14, KLG 3 = 7, and KLG 4 = 2. All participants had knee joint positioning fixed by a lower limb positioner that held the feet externally rotated by 10°; a vertical plate that held the patellae and thighs in line with the tip of the great toes; and the anterior superior iliac spine and greater trochanter positions were fixed for reliability within and between participants [12,13]. Imaging data were reconstructed with 0.37 mm isotropic voxels in a 200 x 350 mm axial field of view with 533 axial frames across the knee joint over a 20 cm scan range from at least the distal femoral diaphysis to proximal tibial diaphysis, and a standard bone kernel. The typical effective radiation dose for each examination was 0.024 mSv, with a volumetric CT dose index of 1.1 mGy and a dose-length product of 22 mGy cm. This effective dose is compared to 0.005 mSv for a plain radiograph set of the knee joint and an average US daily background exposure of 0.008 mSv; one WBCT acquisition is therefore roughly equivalent to 3 days of background radiation [14].

Imaging data sets were previously analyzed using joint space mapping (JSM) as reported by Turmezei *et al.*[4]. In brief, after the distal femur is segmented from the axial imaging data, patches are cut from the femur bone surface object as guided by the shadow of the opposing tibial bone projected back on to the femoral surface. These joint space patches are the framework for the measurement of the distance between the joint bone surfaces (i.e. JSW) using a full-width half-maximum deconvolution of data sampled along a line at the normal to every vertex in the joint space patch mesh. The femoral and tibial articular bony surfaces are thus defined by JSM and contain the same relationship and connectivity of vertices as the original joint space patch mesh [4].

In this study, a new analysis was performed to quantify subarticular bone thickness and trabecular attenuation at these femoral and tibial joint surface patches in 3-D using an endocortical algorithm implementation of cortical bone mapping (CBM) that allows measurement of subchondral, endocortical, and trabecular bone regions along a line at the normal to each vertex at the articular bone surface (Fig. 1) [15]. In this representation, trabecular attenuation is the CBM optimizer algorithm's estimation of the average attenuation value of the bony trabecular network along the line of measurement beneath the joint surface.

Both JSM and CBM were performed using StradView software (version 6.13 [Graham Treece, Cambridge University]; <https://mi.eng.cam.ac.uk/Main/StradView>). The combination of these two techniques allows weight bearing JSW and the subarticular bony parameters of subchondral bone plate thickness (ST), endocortical bone thickness (ET), and trabecular attenuation (TA) at the distal femur (f) and proximal tibia (t) to be co-located vertex-by-vertex on each individual's 3-D joint surface. After registration of the average joint surface (which we call the 'canonical' surface as a reasonable and realistic representation) to each individual's surface, and then transfer of the multiparametric data from each individual onto this canonical, all data was analyzed and presented on the canonical model. All registrations and data transfer to the canonical were performed using wxRegSurf (version 20 [Andrew Gee, Cambridge University]; <https://mi.eng.cam.ac.uk/~ahg/wxRegSurf/>).

Horn's parallel analysis was performed on the results of principal component analysis of the registration vectors and showed that the first three shape modes were responsible for shape mode variation above background noise [16]. A number of parameters were examined: fST = femoral subchondral thickness, fET = femoral endocortical thickness, fTA = femoral trabecular attenuation, tST = tibial subchondral thickness, tET = tibial endocortical thickness, tTA = tibial trabecular attenuation, and JSW. To look at the dependence of each parameter on KLG with SPM, a univariate general linear model was used with an experimental term of KLG (centrally graded in MOST) and confounding terms of age, body mass index, and the first three shape modes to control for effects of systematic misregistration [17,18]. A custom-scripted multivariate implementation of SPM was used to look at the co-dependence of each pair of parameters on the experimental term of KLG, using the SurfStat package (Keith Worsley, McGill University; <https://www.math.mcgill.ca/keith/surfstat/>). Sex was not used in the model because of the correlation with the first shape mode ($r = 0.80$) that represented scale factor. Pearson's correlation coefficient was also calculated vertex-wise on the canonical surface for each of the parameter pairs.

All 20 knees from the 10 participants in the test-retest repeatability study were used for measuring repeatability of all parameters, delivering bias, limits of agreement (LOA) adjusted to allow for more than one knee per individual in the sample [19], and root mean square coefficient of variation where possible, i.e. not with trabecular attenuation which has negative values. The process of spatially co-aligning data on the canonical surface to compare baseline and follow-up values has been previously described [4].

RESULTS

The mean \pm SD age of participants was 57.4 ± 7.2 years, with 23 women and 10 men in the study. All results are displayed on the canonical joint surface model. An example of this model is shown in Fig 2. displaying mean JSW from across the study at the right knee superimposed on the grey distal femur (viewed from below).

SPM revealed that the central-to-posterior medial tibiofemoral joint space was significantly narrowed by up to 0.5 mm with significantly higher tTA by up to 50 attenuation units for each increment in KLG ($p < 0.05$) both alone (Fig. 3, left) and in a wider distribution in combination with multivariate analysis (Fig. 3, right). A small patch at the medial aspect of the lateral joint space also showed significance for JSW alone and JSW-tTA in combination ($p < 0.05$), suggesting that it is modelling medial tibiofemoral joint space loss with subchondral sclerosis along with a medial shift of the femoral condyles with respect to the tibial plateau.

Note that the size of the significant ROIs in the paired JSW-tTA parameter (multivariate) analysis are larger than for either single parameter, meaning that there are some points in the joint space that are only significantly dependent on KLG when parameters are combined. The percentage of the canonical joint space achieving the significance threshold by vertex count increased from a baseline of 16.1% for JSW (lateral/medial = 7.4%/23.6%) and 16.9% for tTA (0%/31.1%) to 33.8% for JSW and tTA

combined (12.7%/51.6%): no other combinations showed such an increase for both parameters, evidencing the strength of their association. There were much smaller regions of significance for JSW and tTA in combination with other parameters, but they were regarded as effects dominated by these already strongly significant single parameters, and none of them showed any increase in percentage coverage value in combination compared to the original single parameters. A full matrix of single and paired parameter SPM results by percentage of significant vertices is shown in Table 1, including the medial and lateral compartment breakdown.

Given theirs being the only stronger paired relationship demonstrated with SPM, for economy of space we show the mean values of the co-dependent factors of JSW and tTA and how they correlate across the joint space in the same KLG category divisions (Fig. 4). The mean distribution maps for all parameters are shown in Figs S1 and S2 categorized as KLG < 2 (n=43) vs KLG = 2 (n=14) vs KLG > 2 (n=9).

Vertex-wise correlation maps in Fig. 4 show that JSW and tTA are more closely correlated with higher KLG category, with the percentage of vertices correlating at $r > |0.50|$ increasing from 2% (KLG < 2), to 11% (KLG = 2), to 30% (KLG > 2). This indicates that these two features become more strongly correlated the worse the radiographic disease, with larger JSW values in the lateral joint space linked to lower tibial trabecular attenuation values, suggesting widening with less sclerosis (or vice versa). There is a more heterogeneous relationship at the medial joint space, predominantly with smaller JSW values linked to larger attenuation values, suggesting narrowing with a mix of more and less sclerosis according to location (or vice versa).

Repeatability for each parameter is presented as average bias from across the whole joint space (Table 2) and best limits of agreement values (Table 3). Full tabulation of repeatability metrics by KLG category, including confidence intervals for limits of agreement and whole joint average root mean square coefficient of variation are included as supplementary Tables S1 to S7. This supplementary material also includes surface distribution maps by KLG category that allow regions to be identified on the joint surface where bias and limits of agreement performance are best (Figs S3 to S9). These visualizations demonstrate that there is variation in repeatability performance across the joint surface, in part due to noise from the small number of participants, but also that the variability is often worse at the joint space margins where misalignment between baseline and follow-up values is likely to have the greatest influence on error [20].

Regarding the repeatability of the absolute values of thickness from Table 3, they are nearly all subvoxel (less than 0.37 mm) in magnitude apart from JSW for the KLG = 2 category. This result appears to be anomalous but is in fact similar in percentage of the mean to many of the other thickness measures that achieve repeatability at around or less than 10% of the mean measure, noting that JSW measures will be nearly one order of magnitude greater than bone thickness (e.g. 1 to 10 mm compared to 0.1 to 1 mm). It also highlights how relatively better the repeatability is for JSW in the KLG < 2 and > 2 categories. The exception to this is for fET, in which repeatability ranges from

12.2% in the KLG < 2 category up to 18.5% in the KLG > 2 category. Note that while attenuation values cannot be expressed as a percentage of the mean (because the attenuation scale has negative values), repeatability variations are nonetheless very small (between 6 and 20 attenuation units) when considering mean bone attenuation values across the joint space are around 300 units.

DISCUSSION

This study has shown it is possible to co-localize 3-D surface based multiparametric measurements across the weight bearing knee joint using cone beam CT imaging, specifically when analyzing JSW and bony parameters such as subchondral plate thickness and trabecular attenuation. We have demonstrated the feasibility of multivariate significance testing in pairs and parameter correlations from both sides of the joint. As a trend, the most recognizable pattern in structural bone depicted by CBM was greater tibial and femoral subarticular bone thickness and attenuation measurements in the medial joint space with worsening Kellgren & Lawrence grade (KLG) category, which could be taken as a quantitative correlate of subchondral sclerosis (Figs S1 and S2). This approach to evaluating subchondral bone with CT has been recognized as having potential for decades[21]. More recently MRI has also been used to analyze this feature [22]. As reported previously, JSM demonstrated greater narrowing of the medial joint space the worse the KLG category [4], which is a staple feature in the radiographic assessment of osteoarthritis. Osteoarthritis can be expected to progress from -0.1 to 0.7 mm per year at the knee in those with radiographically established disease [23].

Yet while joint space narrowing and subchondral sclerosis are well-recognized elements of osteoarthritis, here we have demonstrated 3-D co-localization and quantification of correlation and combined significance testing for their dependence on disease status. This work should prompt further study of their combined strength as predictive parameters. Statistical parametric mapping (SPM) showed that combining JSW and tibial trabecular attenuation (tTA) in paired multivariate analysis increased the surface distribution of their dependence from around 16% to 31% of the joint space and nearly. This was the only pair of parameters to demonstrate strengthened dependence in this fashion. Stronger correlations between these two parameters were noted in individuals with the worst radiological disease, but we also identified little or no correlation between them in a structurally healthy state (according to KLG<2). This suggests that JSW and tTA may become linked when structural disease is established, a relationship that could be explained by the development of subchondral bony sclerosis at sites of cartilage breakdown (or vice versa). The relationship needs further evaluation because the correlation we find in this exploratory study is both strongly positive and negative in the medial joint space. Previous investigation with MRI has shown that baseline subchondral sclerosis is not associated with future cartilage loss in the same knee compartment at either the femoral or tibial aspect [24], but our results suggest that there is an association between joint space loss (whatever the cause) and increased tibial subchondral bone attenuation and, to a less widely distributed extent, subchondral bone plate and endocortical thickness. These relationships warrant further exploration. The fact that no femoral bony parameters met any substantial significance

alone or in combination with JSW (Table 1) may be due to an underpowered analysis since a trend for increased femoral trabecular attenuation was identified with worsening KLG category (Fig. S1).

Repeatability results for thickness parameters were nearly all subvoxel (less than 0.37 mm) in value, demonstrating the ability of our 3-D algorithmic approach to deliver excellent repeatability, with best limits of agreement values nearly all less than 10% of the mean value, apart for fET. This can be explained by the way the algorithm determines the endocortical bone slope (Fig. 1). It is more susceptible to slight variations in the optimization process than for attenuation and JSW measures; because endocortical thickness values are most reliant on this slope, they can therefore be expected to be less repeatable in day-to-day measurements. Future exploration would be of value into whether the endocortical ramp method is the most appropriate to model subchondral bone at the knee joint compared to a standard non-sloped CBM implementation.

We recognize that this study has several limitations. Firstly, attenuation units from CBCT reconstructions are not true Hounsfield Units, with heterogeneity towards the margins of the acquisition and theoretical risk of variability between imaging units [2,25]. For our study, standardized positioning and the same machine, acquisition, and scanning parameters throughout strengthens validity in this respect, but the robust assessment of true attenuation values could be standardized by inclusion of a calibration phantom in follow-on studies, particularly if comparison is required across multiple locations. Secondly, the precise location of the joint space sampling sites will be sensitive to joint space positioning and so a greater degree of assurance of standardized positioning and angulation is strongly advised, e.g. using a construct such as the SynaFlexer Plexiglass positioning frame [BioClinica, formerly Synarc]. We also accept that our convenience study had low numbers (33 individuals, 66 knees), and unevenly distributed KLG categories (KLG < 2 n=43, KLG = 2 n=14, KLG > 2 n=9). Nonetheless, we believe that our results demonstrate statistical significance and associations despite factors that might otherwise detract from their ability to do so. We also recognize the bias introduced by using KLG as the experimental term in the SPM model, because the imaging features that we have quantitatively observed would have been evaluated by radiograph readers to assign KLG. However, we recognize that the two imaging assessments are independent and of inherently different methodologies. In addition, it should also be noted that future studies could equally explore the relationship between quantitative 3-D parameters and other experimental factors such as pain, function, or need for therapeutic intervention such as change in use of analgesic medication or progression to arthroplasty, as well as performing analysis across different time points. We also recognize that using both knees from individuals might introduce an element of duplication bias when they may already be similar, and that we did not perform statistical threshold corrections for the multiple SPM analyses. Nonetheless, we still consider this exploratory research useful in helping to determine prospective evaluation of these parameters for future studies, noting that JSW and tTA were the only two that demonstrated an increased distribution of significance when paired.

CONCLUSION

These findings demonstrate that quantitative measures of 3-D joint space width and tibial trabecular attenuation are repeatable, that they are significantly dependent on radiographic disease severity at the weight bearing knee joint imaged with cone beam CT, and that they are significant not only alone, but also more strongly in combination. This suggests that a multiparametric 3-D approach to imaging assessment of joint space narrowing and subchondral sclerosis in osteoarthritis with CT may lead to improved sensitivity for detecting important structural changes at the knee joint, which could be beneficial for research trials or the evaluation of patients with osteoarthritis in the clinic. Our study has also shown that joint space width and tibial trabecular attenuation had increased spatial correlation with worse radiological disease, a finding that warrants further investigation given that the role of subchondral bone in the progression of osteoarthritis remains poorly understood. We will now be applying these 3-D quantitative techniques in much larger numbers from the Multicenter Osteoarthritis Study in a project designed to determine their ability to predict disease progression and patient-reported outcomes, an important next step in establishing their clinical validity.

ACKNOWLEDGEMENTS

None.

AUTHOR CONTRIBUTIONS

Guarantors of integrity of entire study, T.D.T.; study concepts/study design or data acquisition or data analysis/interpretation, all authors; manuscript drafting or manuscript revision for important intellectual content, all authors; approval of final version of submitted manuscript, all authors; agrees to ensure any questions related to the work are appropriately resolved, all authors; literature research, T.D.T., S.B.L., J.A.L.; clinical studies, N.A.S., J.A.L.; statistical analysis, T.D.T., G.M.T., A.H.G.; and manuscript editing, T.D.T., S.R., G.M.T., A.H.G., J.W.M., J.A.L., K.E.S.P., N.A.S.

ROLE OF THE FUNDING SOURCE

This study was funded by the National Institutes of Health grants to the University of Kansas (R01AR071648–N. Segal), University of Iowa (U01AG18832–J. Torner), University of California-San Francisco (U01AG19069–M. Nevitt) and Boston University (U01AG18820–D. Felson). The funding organization did not have a role in the design, data collection, analysis, or interpretation. The investigators maintained independence in the content of the manuscript and the decision to publish.

CONFLICT OF INTEREST

T.D.T. is a consultant for GlaxoSmithKline. S.B.L. disclosed no relevant relationships. S.R. disclosed no relevant relationships. G.M.T. disclosed no relevant relationships. A.H.G. disclosed no relevant relationships. J.W.M. Activities related to the present article: disclosed no relevant relationships. Activities not related to the present article: has been a consultant for GlaxoSmithKline and Moximed; institution received grants from GlaxoSmithKline and GE Healthcare; received travel assistance from GE Healthcare. Other relationships: disclosed no relevant relationships. J.A.L. disclosed no relevant relationships. K.E.S.P. disclosed no relevant relationships. N.A.S. Activities related to the present

article: CurveBeam loaned a WBCT scanner to the institution without stipulations regarding its use. Activities not related to the present article: consultant for Tenex Health. Other relationships: disclosed no relevant relationships.

REFERENCES

- [1] JW MacKay, JD Kaggie, GM Treece, et al., Three-Dimensional Surface-Based Analysis of Cartilage MRI Data in Knee Osteoarthritis: Validation and Initial Clinical Application, *J Magn Reson Imaging* 52 (2020) 1139–1151. <https://doi.org/10.1002/jmri.27193>.
- [2] MJ Turunen, J Töyräs, HT Kokkonen, JS Jurvelin, Quantitative evaluation of knee subchondral bone mineral density using cone beam computed tomography, *IEEE Trans Med Imaging* 34 (2015) 2186–2190. <https://doi.org/10.1109/TMI.2015.2426684>.
- [3] G Treece, A Gee, Cortical Bone Mapping: Measurement and Statistical Analysis of Localised Skeletal Changes, *Curr Osteoporos Rep* 16 (2018) 617–625. <https://doi.org/10.1007/s11914-018-0475-3>.
- [4] TD Turmezei, S B Low, S Rupret, et al., Quantitative Three-dimensional Assessment of Knee Joint Space Width from Weight-bearing CT, *Radiology* 299 (2021) 649–659. <https://doi.org/10.1148/radiol.2021203928>.
- [5] JT Lynch, MTY Schneider, DM Perriman, et al., Statistical shape modelling reveals large and distinct subchondral bony differences in osteoarthritic knees, *J Biomech* 93 (2019) 177–184. <https://doi.org/10.1016/j.jbiomech.2019.07.003>.
- [6] SS Karhula, MAJ Finnilä, SJO Rytty, et al., Quantifying Subresolution 3D Morphology of Bone with Clinical Computed Tomography, *Ann Biomed Eng* 48 (2020) 595–605. <https://doi.org/10.1007/s10439-019-02374-2>.
- [7] GJ Michalak, R Walker, SK Boyd, Concurrent Assessment of Cartilage Morphology and Bone Microarchitecture in the Human Knee Using Contrast-Enhanced HR-pQCT Imaging, *J Clin Densitom* 22 (2019) 74–85. <https://doi.org/10.1016/j.jocd.2018.07.002>.
- [8] P Omoumi, H Babel, BM Jolles, J Favre, Relationships between cartilage thickness and subchondral bone mineral density in non-osteoarthritic and severely osteoarthritic knees: In vivo concomitant 3D analysis using CT arthrography, *Osteoarthritis Cartilage* 27 (2019) 621–629. <https://doi.org/10.1016/j.joca.2018.12.014>.
- [9] JL Bhatla, A Kroker, SL Manske, CA Emery, SK Boyd, Differences in subchondral bone plate and cartilage thickness between women with anterior cruciate ligament reconstructions and uninjured controls, *Osteoarthr Cartil* 26 (2018) 929–939. <https://doi.org/10.1016/j.joca.2018.04.006>.

- [10] NA Segal, E Frick, J Duryea, et al., Comparison of Tibiofemoral Joint Space Width Measurements from Standing CT and Fixed Flexion Radiography, *J Orthop Res* 35 (2017) 1388–1395. <https://doi.org/10.1002/jor.23387>.
- [11] NA Segal, J Bergin, A Kern, C Findlay, DD Anderson, Test-retest reliability of tibiofemoral joint space width measurements made using a low-dose standing CT scanner, *Skeletal Radiol* 46 (2017) 217–222. <https://doi.org/10.1007/s00256-016-2539-8>.
- [12] NA Segal, MC Nevitt, JA Lynch, J Niu, JC Torner, A Guermazi, Diagnostic performance of 3D standing CT imaging for detection of knee osteoarthritis features., *Phys Sportsmed* 43 (2015) 213–220. <https://doi.org/10.1080/00913847.2015.1074854>.
- [13] NA Segal, J Bergin, A Kern, C Findlay, DD Anderson, Test-retest reliability of tibiofemoral joint space width measurements made using a low-dose standing CT scanner, *Skeletal Radiol* 46 (2017) 217–222. <https://doi.org/10.1007/s00256-016-2539-8>.
- [14] FA Mettler, W Huda, TT Yoshizumi, M Mahesh, Effective Doses in Radiology and Diagnostic Nuclear Medicine: A Catalog, *Radiology Radiological Society of North America*; 248 (2008) 254–263. <https://doi.org/10.1148/radiol.2481071451>.
- [15] RA Pearson, GM Treece, Measurement of the bone endocortical region using clinical CT, *Med Image Anal* 44 (2018) 28–40. <https://doi.org/10.1016/j.media.2017.11.006>.
- [16] JL Horn, A rationale and test for the number of factors in factor analysis, *Psychometrika* 30 (1965) 179–185. <https://doi.org/10.1007/BF02289447>
- [17] KJ Friston, AP Holmes, KJ Worsley, J-P Poline, CD Frith, RSJ Frackowiak, Statistical parametric maps in functional imaging: A general linear approach, *Hum Brain Mapp* 2 (1994) 189–210. <https://doi.org/10.1002/hbm.460020402>.
- [18] AH Gee, GM Treece, Systematic misregistration and the statistical analysis of surface data., *Med Image Anal* 18 (2014) 385–393. <https://doi.org/10.1016/j.media.2013.12.007>.
- [19] JM Bland, DG Altman, Agreement Between Methods of Measurement with Multiple Observations Per Individual, *Journal of Biopharmaceutical Statistics Taylor & Francis*; 17 (2007) 571–582. <https://doi.org/10.1080/10543400701329422>.
- [20] TD Turmezei, GM Treece, AH Gee, R Houlden, KES Poole, A new quantitative 3D approach to imaging of structural joint disease, *Scientific Reports* 8 (2018) 9280. <https://doi.org/10.1038/s41598-018-27486-y>.
- [21] P Rügsegger, B Münch, M Felder, Early detection of osteoarthritis by 3D computed tomography, *Technol Health Care* 1 (1993) 53–66. <https://doi.org/10.3233/THC-1993-1106>.

- [22] JW MacKay, PJ Murray, B Kasmai, G Johnson, ST Donell, AP Toms, Subchondral bone in osteoarthritis: association between MRI texture analysis and histomorphometry, *Osteoarthritis Cartilage* 25 (2017) 700–707. <https://doi.org/10.1016/j.joca.2016.12.011>.
- [23] PS Emrani, JN Katz, CL Kessler, et al., Joint space narrowing and Kellgren-Lawrence progression in knee osteoarthritis: an analytic literature synthesis, *Osteoarthritis Cartilage* 16 (2008) 873–882. <https://doi.org/10.1016/j.joca.2007.12.004>.
- [24] MD Crema, J Cibere, EC Sayre, et al., The relationship between subchondral sclerosis detected with MRI and cartilage loss in a cohort of subjects with knee pain: the knee osteoarthritis progression (KOAP) study, *Osteoarthritis Cartilage* 22 (2014) 540–546. <https://doi.org/10.1016/j.joca.2014.01.006>.
- [25] RWF Vitral, MR Fraga, MJ da Silva Campos, Use of Hounsfield units in cone-beam computed tomography, *Am J Orthod Dentofacial Orthop* 148 (2015) 204. <https://doi.org/10.1016/j.ajodo.2015.05.005>.

FIGURE LEGENDS

Fig. 1 Endocortical CBM uses a ramp model to fit the tail-off from the cortex towards the medulla of the bone. Endocortical thickness (ET) is defined as the width of the ramp, while subchondral bone plate thickness (ST) is defined as the peak thickness plus half of the ramp. This means that the parameters are intrinsically correlated, but also that no specific depth region of interest is required to be pre-set. The overall 1-D line length was 30 mm, sampling from 10 mm outwards from the bone surface to 20 mm inwards. The top graph shows the optimized blur model fit (dashed red line) to the sampled attenuation value data (light blue line), with the ramp deconvolution model fit (solid red line) at a single tibial sample point for an individual from the study with KLG = 0 compared to an individual with KLG = 3 in the bottom graph.

Fig. 2 Example of mean JSW from across all 66 knees in the study shown in situ on the canonical knee joint surfaces (color map) over a right distal femur (grey).

Fig. 3 SPM results from univariate analysis (left column of maps) showing unmasked regions of significantly narrower joint space and greater tibial trabecular attenuation, which become larger in area when combined in the paired multivariate analysis (right column of maps). Joint space width is measured in mm and trabecular attenuation in attenuation units. The significance threshold for unmasked regions is $p < 0.05$, routinely the lower of the two color scale bars, with masked non-significant values represented by the upper color bar.

Fig. 4 Mean JSW and tTA with their correlation map results also broken down KLG < 2 vs KLG = 2 vs KLG > 2.

FIGURES

Figure 1

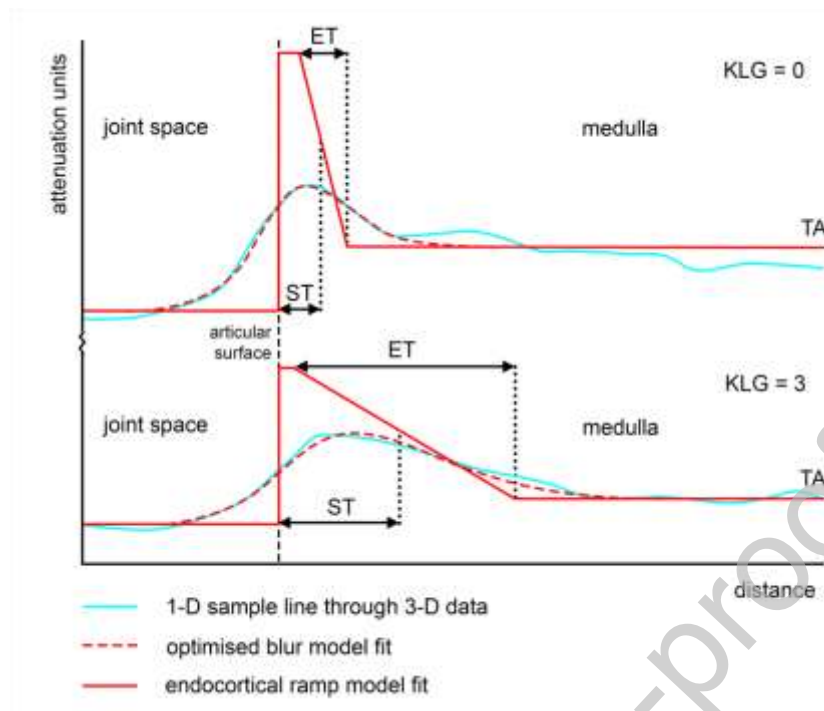


Figure 2

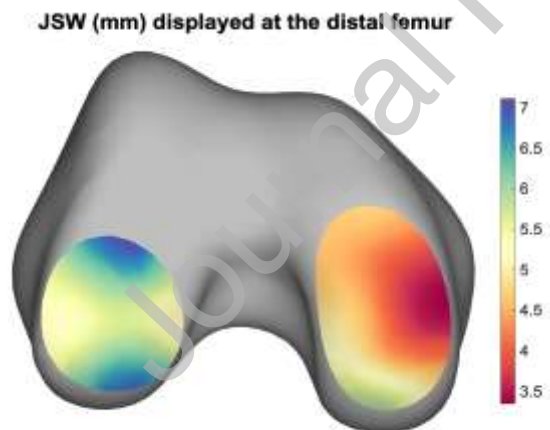


Figure 3

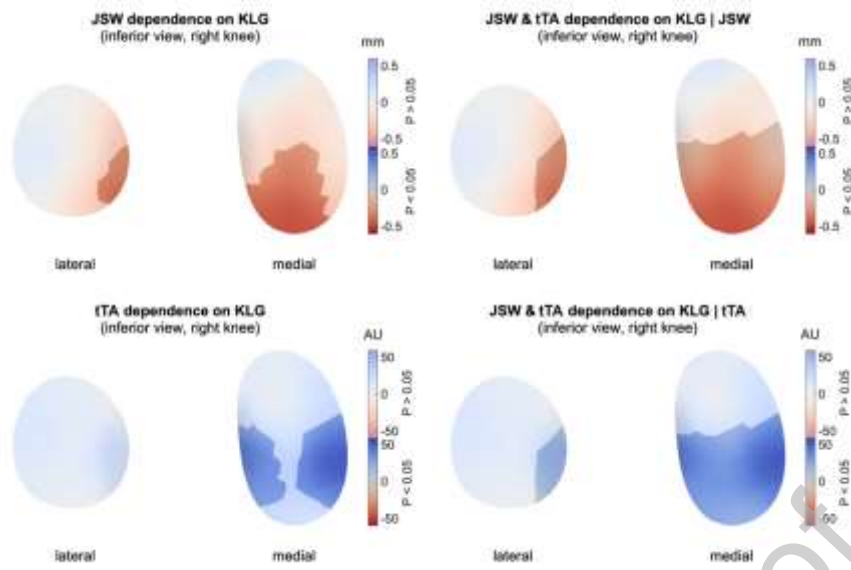
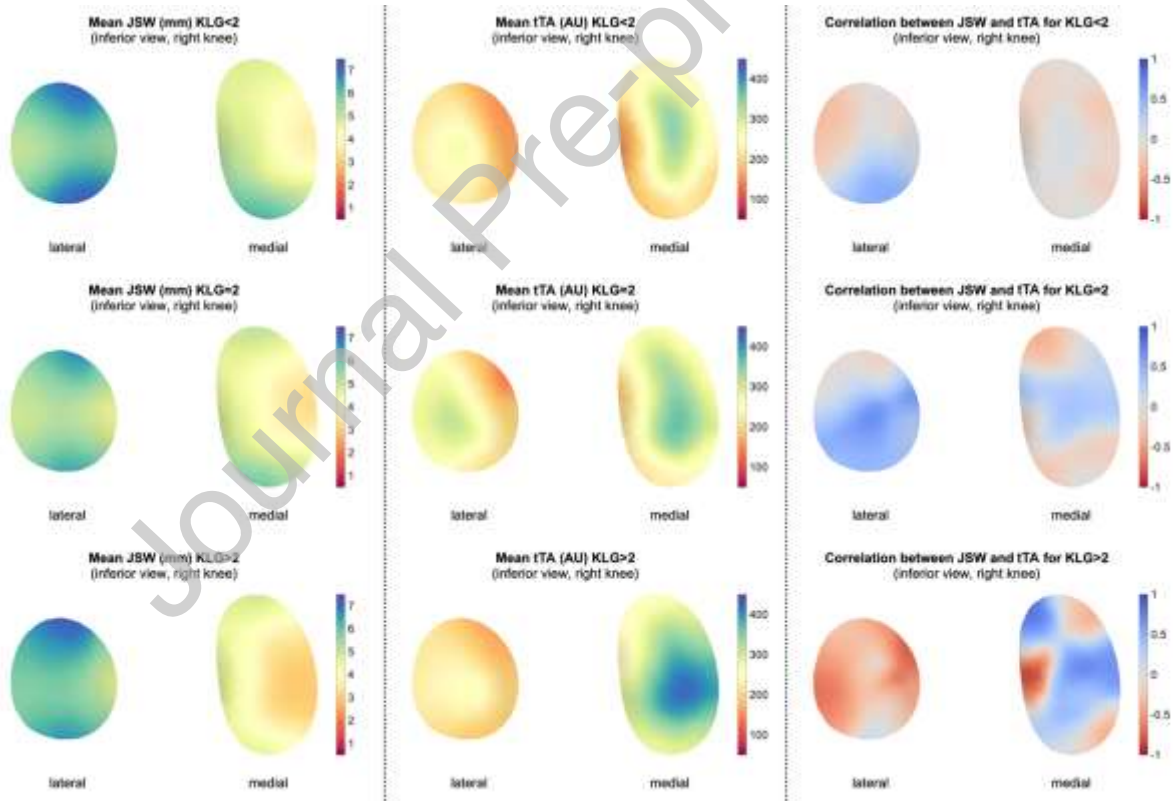


Figure 4



TABLES

Table 1 A matrix of single parameter (along the diagonal) and paired parameter SPM results by % of significant vertices in the canonical patch, $p < 0.05$. The lateral/medial % split is shown in brackets. Any paired results in which there was an increase in percentage value compared to both single parameter results are in bold. Single parameter cells are shaded in grey, pairs with JSW in white, pairs from the same side of the joint in orange, and across the joint space in purple.

%	JSW	fST	fET	fTA	tST	tET	tTA
JSW	16.1 (7.4/23.6)	4.3 (0/8.0)	6.3 (0/11.6)	6.8 (0/12.4)	4.6 (3.2/5.8)	4.8 (3.7/5.8)	33.8 (21.7/51.6)
fST	4.3 (8.0/0)	- (-/-)	- (-/-)	0.5 (0/0.9)	0.2 (0/0.4)	- (-/-)	14.7 (0/27.1)
fET	6.3 (0/11.6)	- (-/-)	- (-/-)	- (-/-)	- (-/-)	- (-/-)	15.9 (0/29.3)
fTA	6.8 (0/12.4)	0.5 (0/0.9)	- (-/-)	0.2 (0/0.4)	1.2 (0/2.2)	1.2 (0/2.2)	15.2 (2.1/26.2)
tST	4.6 (3.2/5.8)	0.2 (0/0.4)	- (-/-)	1.2 (0/2.2)	1.8 (0/1.0)	- (-/-)	11.3 (0/20.8)
tET	4.8 (3.7/5.8)	- (-/-)	- (-/-)	1.2 (0/2.2)	- (-/-)	0.5 (0/0.9)	10.6 (0/19.6)
tTA	33.8 (21.7/51.6)	14.7 (0/27.1)	15.9 (0/29.3)	15.2 (2.1/26.2)	11.3 (0/20.8)	10.6 (0/19.6)	16.9 (0/31.1)

Table 2 Average whole joint space bias for all parameters across grade categories

	KLG<2	KLG=2	KLG>2
JSW (mm)	0.00	0.03	0.06
fST (mm)	0.01	-0.01	0.01
fET (mm)	0.02	-0.02	0.02
fTA (AU)	-1.3	0.0	-1.7
tST (mm)	0.01	0.01	-0.04
tET (mm)	-0.01	0.01	-0.09
tTA (AU)	-0.5	-1.8	-7.8

Table 3 Best limits of agreement for all parameters across grade categories and, where possible, as a percentage of the mean joint surface parameter value.

	KLG<2	KLG=2	KLG>2
JSW (mm)	0.08 (1.7%)	0.40 (7.8%)	0.20 (4.0%)
fST (mm)	0.04 (5.6%)	0.05 (8.2%)	0.02 (3.3%)
fET (mm)	0.10 (12.2%)	0.10 (16.1%)	0.10 (18.5%)
fTA (AU)	11 (-)	11 (-)	6 (-)
tST (mm)	0.06 (4.9%)	0.10 (9.7%)	0.06 (6.3%)
tET (mm)	0.12 (8.2%)	0.12 (10.5%)	0.08 (8.4%)
tTA (AU)	15 (-)	20 (-)	13 (-)

Journal Pre-proof